

in a storage ring. Future uses of this facility include a study of pion production as well as three-body breakup in the d+p system.

1. T. Wise, A.D. Roberts, and W. Haeberli, Nucl. Instrum. and Methods **A336**, 410 (1993).
2. W.A. Dezarn, J. Doskow, J.G. Hardie, H.O. Meyer, R.E. Pollock, B. von Przewoski, T. Rinckel, F. Sperisen, W. Haeberli, B. Lorentz, F. Rathmann, M.A. Ross, T. Wise, P.V. Pancella, contrib. to *Eighth Int. Symp. on Pol. Phen. in Nucl. Phys.*, p. 62.
3. M.A. Ross, A.D. Roberts, T. Wise, W. Haeberli, W.A. Dezarn, J. Doskow, H.O. Meyer, R.E. Pollock, B. von Przewoski, T. Rinckel, F. Sperisen, and P.V. Pancella, Nucl. Instrum. and Methods **A344**, 307 (1994).
4. R.E. Pollock, see elsewhere in this report.
5. B. von Przewoski, H.O. Meyer, P.V. Pancella, S.F. Pate, R.E. Pollock, T. Rinckel, F. Sperisen, J. Sowinski, W. Haeberli, W.K. Pitts, and S. Price, Phys. Rev. **C44**, 44 (1991).
6. B. von Przewoski, W.A. Dezarn, J. Doskow, J.G. Hardie, H.O. Meyer, R.E. Pollock, T. Rinckel, F. Sperisen, W. Haeberli, B. Lorentz, F. Rathmann, M.A. Ross, T. Wise, and P.V. Pancella, Rev. Sci. Instrum. **1**, 67 (1996).

NEAR THRESHOLD PION PRODUCTION VIA ${}^2\text{H}(\vec{p},\pi^0){}^3\text{He}$

A. Betker, J. Cameron, W. Jacobs, H. Nann, T. Peterson,
J. Shao, M. Spraker, J. Szymanski, S. Vigdor, and K. Warman
Indiana University Cyclotron Facility, Bloomington, Indiana 47408

W.K. Pitts
University of Louisville, Louisville, Kentucky 40292

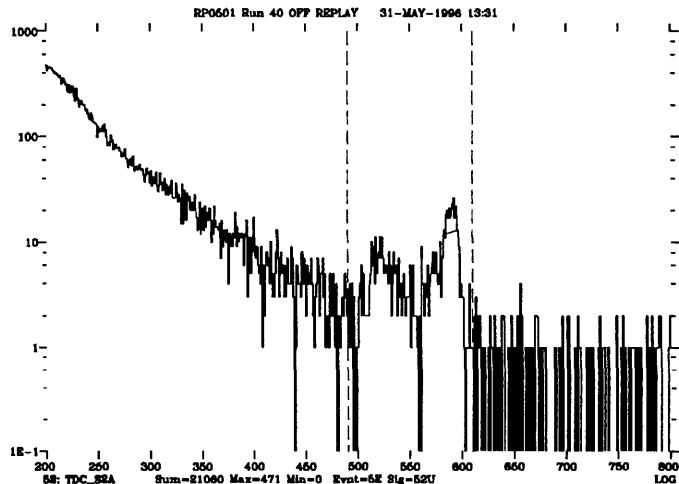
Reactions of the class (N, π) have generated renewed interest because the high momentum transfer (necessary to knockout a virtual pion) selects short range aspects of the NN interaction. Furthermore, it is expected that close to the pion-production threshold these reactions proceed in a non-resonant mode; that is, a real intermediate $\Delta(1232)$ which subsequently decays into a nucleon and a pion is not produced. Two previous experiments have examined the reaction ${}^2\text{H}(p,\pi^0){}^3\text{He}$ near threshold. One of these was performed at IUCF¹ and the other at Saclay.² The results from these experiments show important discrepancies. The general trend of cross section σ versus $\eta \equiv p_{cm}/m_\pi$ is linear for the Saclay data but has a downward concavity for the IUCF data. Thus, the values of σ are not in agreement (in general) for a given η . The largest difference in the value of σ is for the highest η of the IUCF data set, $\eta = 0.20$:

IUCF Measurement	$2.37 \pm 0.07 \mu\text{b}$,
Saclay Measurement	$3.20 \pm 0.04 \mu\text{b}$.

Weak interference between s-wave and p-wave production would produce an upward concavity for σ versus η . Thus both experiments imply strong interference between these partial waves, but at different strengths. However both data sets are consistent with results from pion absorption experiments.^{3,4}

To help resolve questions about these discrepancies, experiment CE58 was performed to measure the differential cross sections and analyzing powers for the reaction ${}^2\text{H}(\vec{p}, \pi^0){}^3\text{He}$ at energies near the pion production threshold. The pions were not directly observed; instead the recoiling ${}^3\text{He}$ nuclei were detected to identify the reaction. The T-Region Magnetic Channel was employed to separate the ${}^3\text{He}$ nuclei cleanly from the background of scattered protons and deuterons in two ways. First, the elastically scattered protons and deuterons were outside the channel's rigidity acceptance. Second, the 5.7-m flight path down the channel allowed velocity selection from time of flight (TOF) information as shown in Fig. 1. The channel was instrumented with a thin plastic scintillator (S1) and a drift chamber (DC) at the channel entrance, and a delay-line chamber and thick plastic scintillator (S2) at the channel exit. A set of four plastic scintillators and a (one dimensional) silicon position-sensitive detector were used to monitor the luminosity by observing p-d elastic scattering. The G-Region polarimeter was used to monitor the beam polarization at the end of each Cooler cycle via p- ${}^{12}\text{C}$ scattering.

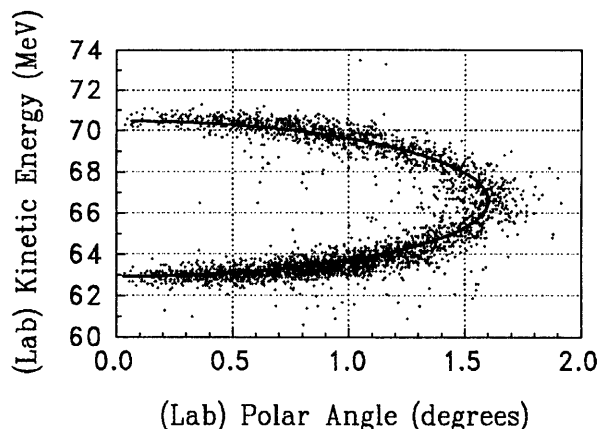
Figure 1. An example of a raw TOF spectrum. The trigger requirement was a coincidence between S1 and S2. The ${}^3\text{He}$ group lies between the dashed lines. The peaks on each side of the distribution correspond to ${}^3\text{He}$ nuclei going forward (left edge) and backward (right edge) in the center-of-mass frame.



Selection of the ${}^3\text{He}$ events was accomplished with a cut on pulse height in S1 as well as a cut on the correlation between TOF and pulse height from S2. For one of the runs, the data taken in November 1995, another scintillator S3 was placed behind S2. Signals from S3 allow a test of the cleanliness of the previously mentioned cuts, because S2 is thick enough to range out all of the ${}^3\text{He}$ nuclei. The TOF provides an energy measurement for the ${}^3\text{He}$ and the DC provides two dimensional position information that allows determination of the laboratory-frame scattering angles. The signature of pion production is the proper correlation from two body kinematics between the energy and the (laboratory) polar angle for the observed ${}^3\text{He}$, as shown in Fig. 2.

The configuration of the channel's beamlines and magnetic fields creates a geometrically limited and non-uniform acceptance. The probability for transmission through the channel

Figure 2. The correlation between the laboratory polar angle and the kinetic energy for ^3He nuclei. The solid curve is determined from two body kinematics, known masses, and a known beam energy of 200.5 MeV.



depends on (at least) three variables for each incident particle: the rigidity, and the two position coordinates in the front wire chamber. Data for pion production had to be taken in several “bites”; both the momentum setting and the laboratory angle of the channel were changed to cover different parts of the phase space for the ^3He . Note that Fig. 2 displays data from a single setting of the channel’s angle and momentum.

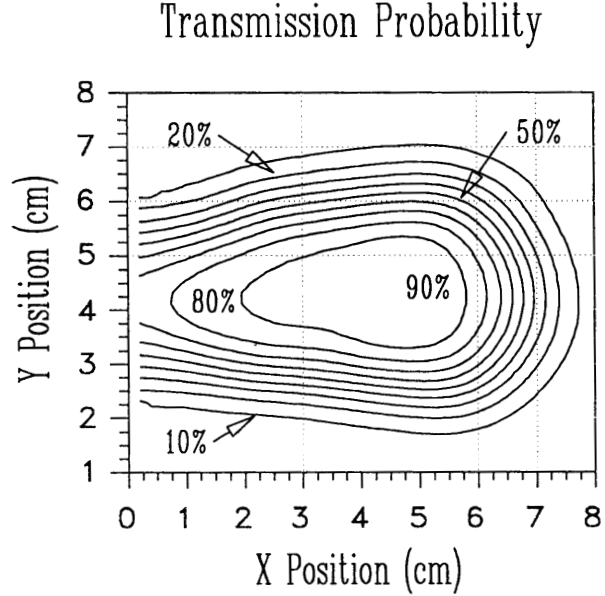
In order to normalize the differential cross section properly, the magnetic-channel transmission function was measured. These measurements used proton elastic scattering from ^1H and ^{12}C targets for three beam energies that gave the protons similar rigidity to the ^3He nuclei from pion production. Furthermore, the channel magnets were set to several scalings of the magnetic-tune solution. This gave the transmission as a function of *relative* rigidity that is defined as the ratio of the channel’s central momentum setting to the beam’s momentum. To measure the transmission for a given energy and momentum setting, the flux of elastically scattered protons at the channel entrance and the flux at the channel exit were both measured. Two plastic scintillators on beam right were used to monitor the luminosity and permit normalization between measurements of the flux at the entrance and exit. The probability of transmission for a specific momentum setting is shown as a function position on the entrance wire chamber in Fig 3.

Table 1

η	Run	Approximate number of ^3He events
0.08	CE58A	10,000
0.13	CE58B	7,000
0.17	CE58A	5,000
0.24	CE58A	5,000
0.32	CE58B	4,000

At this time, the CE58 data set is complete and will provide differential cross sections and analyzing powers for five different pion momenta near the production threshold (see Table 1). Work that remains to be done includes energy-loss calculations to match the

Figure 3. The probability of transmission through the T-Region channel as a function of position on the entrance wire chamber for a specific setting of the channel. The innermost contour corresponds to 90% transmission; each successive contour corresponds to 80%, 70%, ..., 10%. The orientation corresponds to the wire chamber as viewed from the target position.



proton rigidities from the transmission measurements to the rigidities of the ^3He nuclei from pion production. After determining the acceptance for ^3He nuclei for each channel setting (both for varied angle and for varied momentum setting), data from each setting need to be normalized and position-matched in order to produce a complete data set for each pion momentum. Finally, data from the polarimeter will be analyzed and used to normalize rates for each spin state in order to determine analyzing powers.

1. M. A. Pickar, Ph.D. Thesis, Indiana University, 1982.
2. A. Boudard *et al.*, News from Saturne, **17** (1993).
3. V. N. Nikulin *et al.*, 1996 preprint
4. M. A. Pickar *et al.*, Phys. Rev. C **46**, 397 (1992).